Research Paper

Numerical and Analytical Solution of Low-Density Lipoprotein Deposition in A Curved Arterial Wall Using Multilayer Model

H. Tamim [*]

Department of Mechanical Engineering, Arak Branch, Islamic Azad University, Arak, Iran

ABSTRACT

The transport of macromolecules, such as low-density lipoproteins (LDLs), and their abnormal accumulation within the arterial wall plays an important role in formation and development of atherosclerosis. In this study, the numerical-analytical solution of the LDL mass transfer in lumen-wall of a 3D curved artery is investigated. The governing equations consist of, continuity, momentum conservation and the LDLs mass transfer equations are solved based on appropriate boundary conditions and the results are obtained in the form of main and secondary flow velocity field contours, shear stress profiles, concentration and penetration rate of the LDLs into the wall. In this investigation, a new model of the arterial wall, named multilayer model, was used. According to the results, because of centrifugal forces and formation of secondary flows, an increase in surface concentration and penetration rate at the inner part was seen compared with outer part. Also, the reduction of Reynolds number and curvature ratio will augment the LDLs accumulation at the arterial wall.

Keywords: LDL Mass deposition; Atherosclerosis; Curved artery; Multilayer model.

1   INTRODUCTION

ATHEROSCLEROSIS is one of the most common types of cardiovascular disease, occurring mainly in large and medium-sized arteries [1]. Abnormal transport and accumulation of macromolecules such as low-density lipoproteins (LDL) is considered to be one of the main causes of this condition [2, 3]. The accumulation of these molecules causes the narrowing of the cross-sectional area of the vessel, resulting in its occlusion [4].

_____
[*]Corresponding author. Tel.: +98 086 34132270.
E-mail address: hossein.tamim@iau.ac.ir (H. Tamim)
.

JOURNAL OF SOLID MECHANICS JSM

It is shown that the hemodynamics of the vessels play an effective role in the formation and development of the vascular occlusion. Therefore, the coronary and carotid arteries with their curved and bifurcated geometries have attracted the attention of many researchers [5-10]. Prosi et al. in 2005 listed three different models for simulating the vessel wall [11]. In the simplest model, the vessel wall is replaced by a simple boundary condition [12]. In another model, the mass transfer of particles in the vessel wall is simulated by a simple mass transfer coefficient [11]. The most realistic model is the multilayer model, which is more consistent with the physiological nature of the blood vessel structure. In this model, the vessel wall is considered to consist of several distinct layers with different properties [13, 14]. The innermost layer of the vessel is called the intima, which is covered by a single endothelial cell membrane. This single-cell membrane is located between the blood flow and the vessel wall. The next layer is called the internal elastic layer (IEL), which is made of an impermeable tissue with small pores, and the outermost layer of the wall, called the media, is made of muscle and elastic cells. The distribution of LDL particles on the vessel wall and consequently in the layers of the wall is of great importance. The abnormal accumulation of these particles in the intima layer and their oxidation cause the activation of monocytes and macrophages, resulting in their absorption and the formation of the initial nuclei of the vessel occlusion plaques [15].

In general, researchers have used two experimental and computational methods to study the transport of LDL particles. The first method is based on animal experiments, which, despite its strengths, has some drawbacks, including common diseases between humans and animals [16]. In 2013, Zai et al. tested the effect of flow field and LDL particle concentration on the location of artery occlusion in a rabbit [17]. Some researchers have used analytical methods in simpler geometries or with simplifying assumptions. In 2008, Khakpour and Vafaei [10] and Yang and Vafaei [18] investigated and studied a straight artery in two separate studies. Recently, Wang and Vafaei [4] used an analytical method in a curved artery. In this study, they used a second-order polynomial approximation for the concentration distribution profile in the boundary layer and assumed that the curvature of the vessel had no effect on the particle concentration in a given cross-section.

In more complex geometries, the use of numerical methods is unavoidable [19]. In 2018, Roustai et al. [20] used a numerical solution technique to investigate the effect of structure-fluid interaction in a multilayer model. Bocak et al. [21] and Touri et al. [22] used the latter technique to study curved arteries. The non-Newtonian effect of blood flow in the human aortic artery was evaluated and quantified by Liu et al. in 2011 [23] and the effect of the arterial flow field on changes in mass transfer rate and macromolecule concentration by Diranlu et al. [24] in 2015.

In 2017, Iasiello et al. [25] investigated the combination of mass transport of components in the wall and the artery lumen in the aorta-pelvic bifurcation geometry. In 2013, Rabi et al. [26] conducted a numerical study based on the finite volume method to investigate the effects of non-Newtonian and pulsatile blood flow on mass transport of components in the presence of vessel occlusion. They showed that the wall shear stress in the middle of the occlusion is very detrimental, and then a reverse pressure gradient will appear due to the return flow. In 2002, Wada and Carino [27] numerically evaluated the effect of the flow field in an artery with several different curvatures on the wall shear stress and the distribution of LDL concentration at its interface. More recently, in 2019, Tamim et al. [28] investigated the effect of the length of the initial artery organelle on the flow field and the boundary layer characteristics of LDL concentration. In their study, they focused only on the vessel lumen and used the second model to simulate the arterial wall. They showed that straighter vessels with lower Reynolds numbers have a greater potential for particle aggregation, with about a 1 to 2 percent increase in concentration at the wall compared to free-flowing blood.

In many studies, wall shear stress has been considered a very important factor in the formation of artery occlusion. Shear stress affects the particle concentration and this condition often starts in areas with lower shear stress. Therefore, finding a relationship between wall shear stress and LDL particle concentration has attracted the attention of many researchers. In 2015, Jesionek and Kaster [29] evaluated the effect of shear stress on LDL transport in the wall of an artery. Their study indicated an inverse relationship between shear stress and particle concentration. The effect of stress and spiral flow in coronary arteries was studied in 2018 by Nisko et al. [30]. They found that the spiral structure of the flow determines the velocity field, which is affected by the geometry of the vessel. In addition, they showed that the minimum shear stress occurs at the position of maximum spiral flow intensity. Recently, numerous studies have been conducted to study the effect of various parameters and biological conditions on the flow field and LDL concentration, such as non-Newtonian effect [9, 31], structure-fluid interaction [24, 32], hyperthermic and hypothermic effect [33], and pulsatile flow on the length of the primary organelle [34].

In view of the above, despite the research conducted in the field of LDL particle mass transfer in the blood, no study has been conducted on the exact solution of its concentration distribution in the boundary layer of a curved artery and its combination with the analytical solution in different layers of the vessel wall using a multilayer model that has an important effect on the formation of vessel occlusion. It should be noted that in the study conducted by Wang and Vafai [4], which is the closest study to the present work, the concentration distribution was assumed to be

a quadratic function with uncertain coefficients, such that at a certain point, the curvature of the vessel will not have any effect on the concentration distribution. However, in the present paper, in addition to all the physiological conditions used in the study by Wang and Vafai, these two simplifying approximations are discarded and an exact solution for the concentration at each point of a curved three-dimensional vessel is obtained; which makes the complexity of the solution much greater but closer to the real conditions.

In this study, the transport of LDL particles in steady and laminar flow in a 120-degree curved artery without occlusion, in the three-dimensional case, incompressible flow and Newtonian fluid, has been numerically solved. Also, the equations governing the transport of LDL in the vessel wall and the flux rate of particles penetrating into it have been solved by considering a new multilayer model. For the first time in this study, the effect of various parameters such as vessel curvature and Reynolds number on the precise concentration distribution in a cross-section of a curved artery has been measured and evaluated.

It should be noted that the written numerical program is also capable of solving flow equations in a pulsatile manner, and the selection of an appropriate time step acts as a tool in numerical stability. Therefore, the achievements of the present study are very important and complement previous valuable research in identifying and predicting the points prone to occlusion in blood arteries. In the following, the effect of geometric, hemodynamic and physiological parameters on the distribution of LDL concentration, its penetration rate and areas prone to occlusion is presented in detail.

2 THE MATHEMATICAL MODEL

2.1 Physical Model

Figure 1 shows a schematic illustration of a 120° curved left coronary artery with an internal diameter of D = 1/3 mm and a wall thickness of 214 μm. The curvature ratio of this vessel is δc = 0.1. In order to simplify the simulation, it is assumed that the cross-sectional area of the vessel at different points is a circle with a constant radius. In the numerical program written to extract the results for a straight vessel, a very small curvature ratio (δc = 0.01) is used. In this study, the Reynolds number is Re = 245, the Schmidt number is Sc = 1/2×105 [4 and 8], and the flow is considered to be steady, incompressible, and Newtonian fluid.

Considering the geometry under study, the most appropriate coordinate system is the toroidal coordinate system, whose components are r, θ, and φ, respectively. The mutual relationships between the components of this system and the Cartesian coordinate system are expressed as follows:
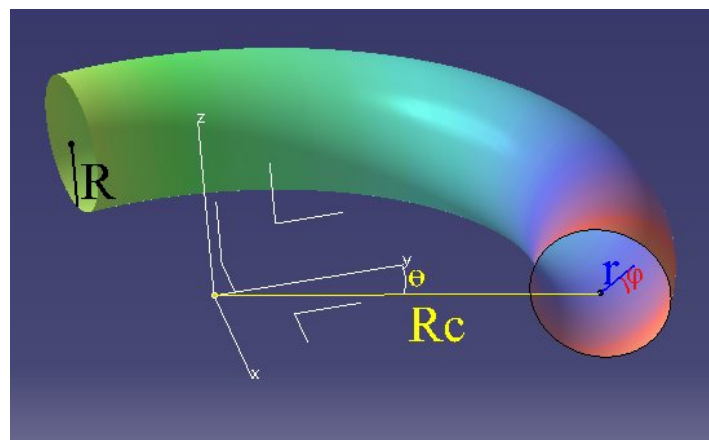

Fig. 1
120° curved artery geometry.

$$\begin{pmatrix} r \\ \theta \\ \varphi \end{pmatrix} = \begin{pmatrix} \sqrt{\left(\sqrt{x^2+y^2}-R_c\right)^2+z^2} \\ \tan^{-1}\dfrac{z}{\sqrt{x^2+y^2}-R_c} \\ \tan^{-1}\dfrac{y}{x} \end{pmatrix} \tag{1}$$

$$\begin{pmatrix} x \\ y \\ z \end{pmatrix} = \begin{pmatrix} \left(R_c+r\cos(\theta)\right)\cos\varphi \\ \left(R_c+r\cos(\theta)\right)\sin\varphi \\ r\sin\theta \end{pmatrix} \tag{2}$$

2.2 Governing Equations

To obtain the distribution of LDL concentration in the blood, first the velocity field in the vessel channel must be determined and then the mass transfer equations must be solved using it. Therefore, the governing equations in the vessel channel include the continuity equation, conservation of momentum, and mass transfer as follows:

$$\nabla \vec{V}' = 0 \tag{3}$$

$$\rho\frac{\partial \vec{V}'}{\partial t} + \rho\vec{V}'.\nabla \vec{V}' = -\nabla p' + \mu\nabla^2\vec{V}' \tag{4}$$

$$\frac{\partial c'}{\partial t} + \vec{V}'.\nabla c' = D_e\nabla^2 c' \tag{5}$$

The boundary conditions of the above equations are as follows: at the vessel inlet, the velocity profile is developed and at its outlet, a zero velocity gradient is considered. Also, at the vessel wall interface, the no-slip condition is valid for the two velocity components and the filtration velocity for the radial component. Regarding the boundary conditions of the concentration equation, a reference concentration of $c_0 = 28.6 \times 10^{-3}$ nmol/mm^3 for the inlet and a zero gradient for the outlet and a balance of convective, diffusive and introduced fluxes into the vessel are applied [4].

In this study, a four-layer model was used to study the mass transfer of LDL particles in the arterial wall. In this regard, the vessel wall was considered to consist of four layers including endothelium, intima, IAL, and media. To obtain the distribution of LDL concentration in the vessel wall, an analytical solution was used by applying the following assumptions:

a) Due to the transverse pressure gradient, the axial and secondary velocities in the vessel wall are negligible.

b) Due to the negligible thickness of the wall compared to the diameter of the vessel (ratio of approximately 0.06), the arterial wall can be considered directly.

Using the above assumptions, the mass transfer equation in the three layers of endothelium, intima, and IAL will be as follows:

$$B\frac{\partial c}{\partial r^+} = E\frac{\partial}{\partial r^+}\left(r^+\frac{\partial c}{\partial r^+}\right) \tag{6}$$

The general solution is as follows:

$$c\left(r^+\right) = C_1^i \times \frac{E_i r^{+\frac{B_i}{E_i}}}{B_i} + C_2^i \tag{7}$$

In the media layer, considering an irreversible first-order chemical reaction, the mass transfer equation and its general solution are obtained as follows:

$$\frac{B_4}{r^+}\frac{\partial c}{\partial r^+} = E_4 \frac{1}{r^+}\frac{\partial}{\partial r^+}\left(r^+\frac{\partial c}{\partial r^+}\right) - kc \tag{8}$$

$$c\left(r^+\right) = C_1^4 \times r^{+\frac{B_4}{2E_4}} I_{\frac{B_4}{2E_4}}\left(\frac{\sqrt{k}}{\sqrt{E_4}}r^+\right) + C_2^4 \times r^{+\frac{B_4}{2E_4}} K_{\frac{B_4}{2E_4}}\left(\frac{\sqrt{k}}{\sqrt{E_4}}r^+\right) \tag{9}$$

In equations (7) and (9), I and K are the modified Bessel functions of the first and second kind, respectively, and C_i are eight constants related to the general solution in the four wall layers, which can be calculated by applying the boundary conditions of concentration and its mass flux as follows at the interface between the layers and also in the vessel channel.

$$c\left(r\right)\Big|_+^0 = c\left(r\right)\Big|_-^0 \tag{10}$$

$$\left[Bc - Er\frac{\partial c}{\partial r}\right]\Big|_+^0 = \left[Bc - Er\frac{\partial c}{\partial r}\right]\Big|_-^0 \tag{11}$$

In order to make the governing equations dimensionless, the following dimensionless parameters have been used:

$$r = \frac{r'}{D}, \quad u = \frac{u'}{w_m}, \quad v = \frac{v'}{w_m}, \quad w = \frac{w'}{w_m}, \quad p = \frac{p'}{\rho w_m^2}, \quad t = \frac{t'}{D/w_m},$$

$$Re = \frac{w_m D}{v}, \quad Sc = \frac{v}{D_e}, \quad Dn = 2\sqrt{\delta_c}Re, \quad c = \frac{c'}{c_0} \tag{12}$$

In the above equations, r represents the radial component, D is the diameter of the artery, u is the dimensionless component of the velocity in the radial direction, wm is the average axial velocity, v is the dimensionless component of the velocity in the circumferential direction, w is the dimensionless component of the velocity in the direction of curvature, p is the dimensionless pressure, ρ is the density, t is the dimensionless time, Re is the Reynolds number, v is the kinematic viscosity, Sc is the Schmidt number, D_e is the LDL mass diffusion coefficient, Dn is the Dean number, δc is the curvature ratio, c is the dimensionless concentration, and c_0 is the input reference LDL concentration. The values of the parameters used in the above equations are presented in Table 1.

In this paper, the image method first introduced by Chorin [35] for solving the momentum conservation equations is used. In this regard, the system of governing equations is decomposed by a second-order finite difference scheme in a forward-in-time and central-in-space manner. Although, in this method the transient response is also physically correct, in this study the focus is on the steady-state response in which the transient terms have been eliminated. In order to obtain the physical pressure field, a non-uniform displaced grid with no nodes located on the boundaries and much denser in the vicinity of the wall is used. It should be noted that in the written computational program, a maximum residual error of order 6-10 is considered to achieve the steady-state solution.

Table1
Values of physiological blood parameters and LDL.

Parameter	Value	Ref.
Artery Diameter (D)	3.1 mm	[18]
Filtration Velocity (V_w)	2.31×10^{-5} mm/s	[27]
Mean Axial Velocity (w_m)	169 mm/s	[4]
Inlet LDL Concentration (c_0)	28.6×10^{-3} nmol/mm^3	[4]
Reynolds Number (Re)	245	[4]
Schmidt Number (Sc)	1.2×10^5	[8]
Density (ρ)	1.057×10^{-3} g/mm^3	[3]
Diffusion Coefficient (D_e)	2.87×10^{-5} mm^2/s	[4]
Dynamic Viscosity (μ)	3.70×10^{-3} g/mms	[4]

The LDL mass transport equations in the blood flow channel and the vessel wall are related using the boundary condition of continuity of concentration and flux at the blood flow channel-wall interface. According to the Chorin algorithm, at each time step, first the auxiliary velocity field (defined by breaking the momentum conservation equation) is obtained, then the pressure field is determined from the solution of the Poisson pressure equation using one of the appropriate linear system solving methods, and finally the new values of the velocity and concentration fields are calculated and the next time step begins.

3   VALIDATION OF THE NUMERICAL METHOD

To verify the accuracy of the method used in solving the governing equations, due to the lack of a comprehensive and appropriate laboratory study, the closest existing numerical and experimental works to the present study in terms of geometric and physiological conditions have been selected.

For this purpose, the results of the present numerical method have been compared with the analytical and numerical results presented by reputable references. It is worth noting that this comparison can indicate the accuracy of the numerical method and analytical modeling of LDL particle mass transfer in the wall of a curved coronary artery.

Table 2
Comparison of particle concentrations with existing corresponding results.

Parameter	Ref. [11]	Ref. [3]	Present Study
Filtration Velocity	1.76×10^{-5}	2.31×10^{-5}	2.31×10^{-5}
Surface Deposition	1.0262	1.0246	1.025
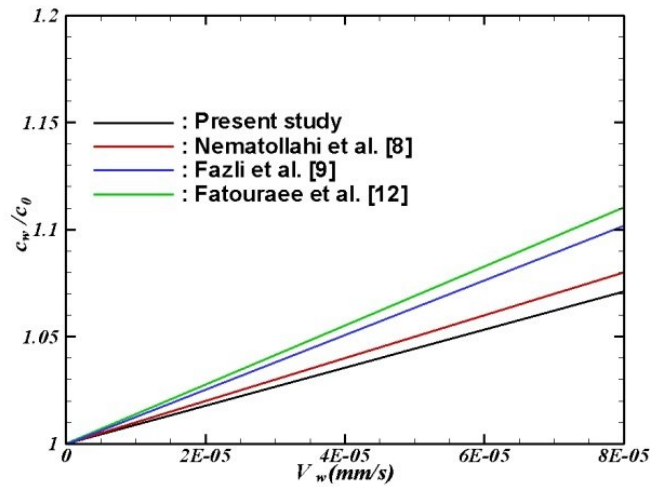
Fig. 2
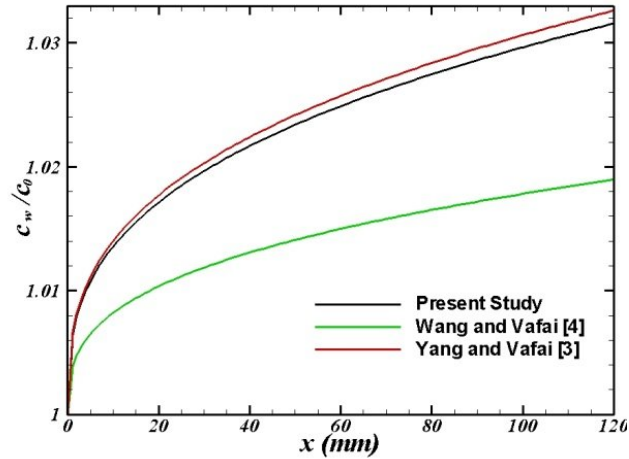Comparison of changes in surface concentration of LDL particles versus filtration rate.

Fig. 3
Comparison of changes in surface concentration of LDL particles along the artery axis**.**

It should be noted that in the study by Wang and Vafai, the concentration distribution was considered with two approximations. First, despite the presence of concentration curvature in a cross-section, it should be completely uniform and second, the concentration distribution function should be a quadratic function. In the present study, for the purpose of validation, all geometric and physiological conditions similar to the models used in these studies have been selected.

Figures 4 to 7 show a comparison of the distribution of LDL particle concentrations in the radial direction at the end of the vessel in the different layers constituting the arterial wall, which indicates a favorable agreement between the results obtained and the results of corresponding studies. It is observed that the difference between the models used decreases with advancing towards the outside of the vessel wall and the slope of the concentration distribution graph becomes horizontal at the end of the media layer, indicating that the mass transfer rate from this layer to the adjacent tissue is zero.
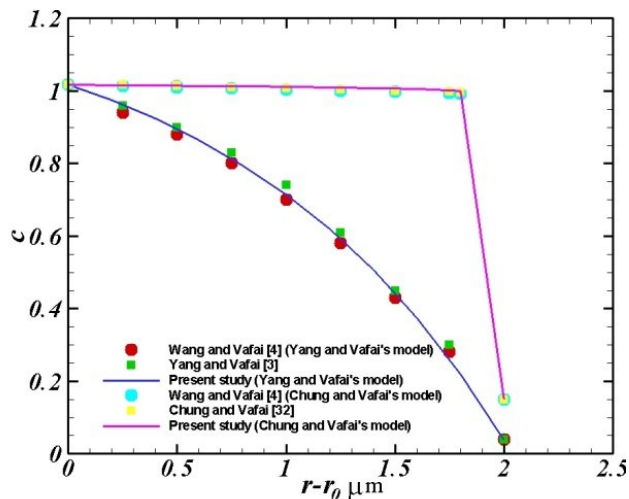
Fig. 4
Comparison of the radial distribution of LDL concentration in the endothelial layer.
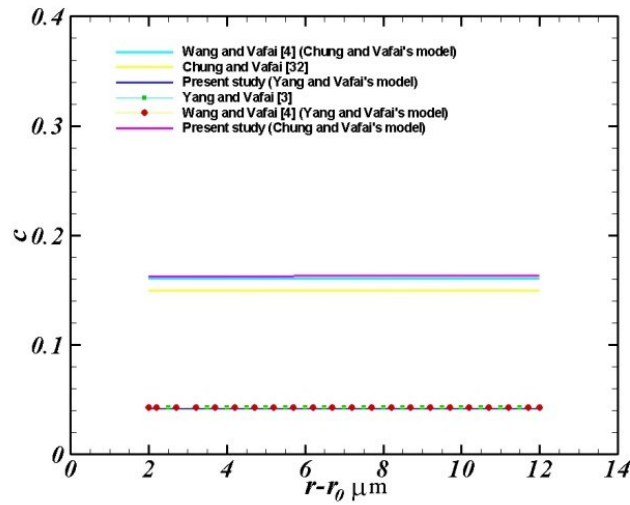
Fig. 5
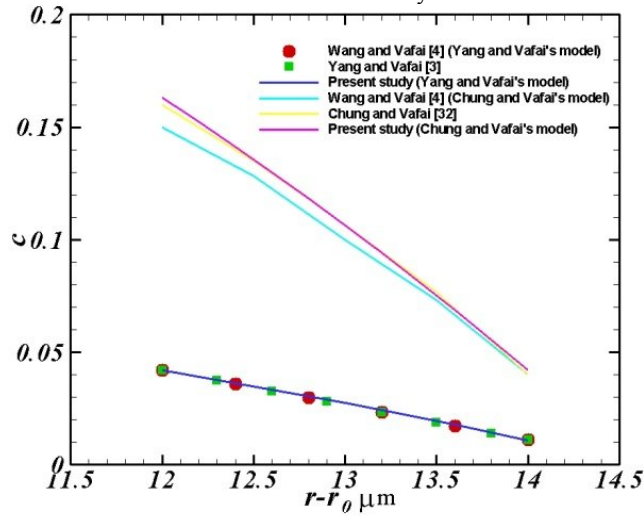Comparison of the radial distribution of LDL concentration in the intima layer**.**

Fig. 6
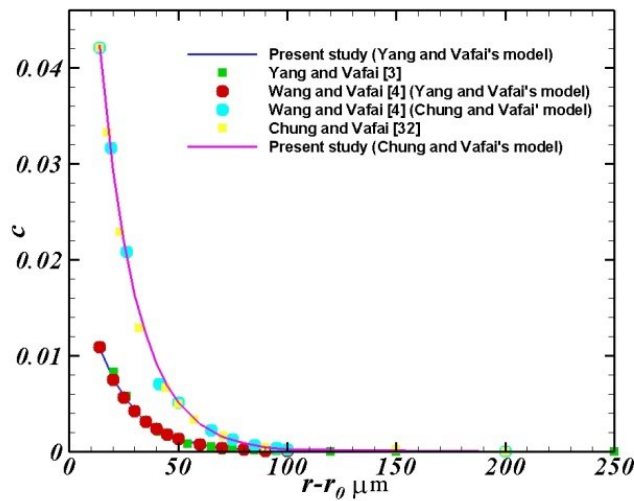Comparison of the radial distribution of LDL concentration in the IEL layer.

Fig. 7
Comparison of the radial distribution of LDL concentration in the media layer**.**

4   GRID INDEPENCY

In order to investigate the independence of the computational grid of the written numerical code, grids with multiple sizes have been studied. The results for three different sizes in the form of wall shear stress, LDL surface concentration, maximum velocity and axial velocity contour for the developed region of a curved artery with a curvature ratio of 0.1 are presented in Table 3. Numerous numerical studies indicate that the optimal values of grid points in the radial, circumferential and axial directions are 60, 35 and 50, respectively, so that a maximum error of about 1.5% is generated.

Table 3
Independence from computational grid: shear stress, surface concentration, maximum velocity and axial velocity contour.

Grid Size	τ_w	c_w	w_{max}	Axial velocity contour
30×20×30	13.8145	1.0151	1.9873	
40×25×40	13.8341	1.0167	2.0072	
60×35×50	13.8356	1.0168	1.9996	

5   RESULTS AND DISCUSSIONS

In curved vessels, due to the complexity of the flow behavior due to centrifugal forces, a detailed study of the flow field is absolutely necessary. Therefore, first, the main and secondary velocity fields inside the geometry under consideration (Figure 1) are studied, and then the distribution of LDL concentration in different geometric and physiological states, as well as the mass flux rate penetrating the wall, are investigated.

5.1 Lumen

In this section, in order to study the complexities of flow in bends, the axial velocity field and secondary flow are investigated for Reynolds number 245. Figure 8-a shows the progression of axial velocity contours and Figure 8-b shows the formation of secondary flow lines along the bend of the vessel for every 30 degrees. According to Figure 8, at the beginning of the bend of the vessel, the flow has a slight deviation from the symmetry state. Gradually, as the flow progresses and centrifugal forces develop, the particles, after colliding with the outer wall from the upper and lower half-planes, return to the inner wall of the bend, which causes the formation of a secondary flow perpendicular to the main flow in the bend. These secondary flows, which are called secondary Dean flows, also include a pair of vortices with opposite directions, which is clearly visible in Figure 8-b. The effect of artery curvature on the axial velocity field and secondary flow is shown in Figures 9a and 9b, respectively. As the vessel becomes more curved, the tendency of particles to move away from the center of curvature increases, and as a result, the position of the maximum axial velocity shifts. Therefore, the velocity gradients in the vicinity of the outer wall of the bend increase and more shear stresses will result. According to Figure 9b, the center of the secondary flow vortices changes location with the curvature of the vessel, which is a very important hemodynamic phenomenon. In vessels with very small curvature, the very weak secondary flows rotate approximately around the angle φ = 270° and 90°. However, as the vessel becomes more curved, this angle decreases to 45°.

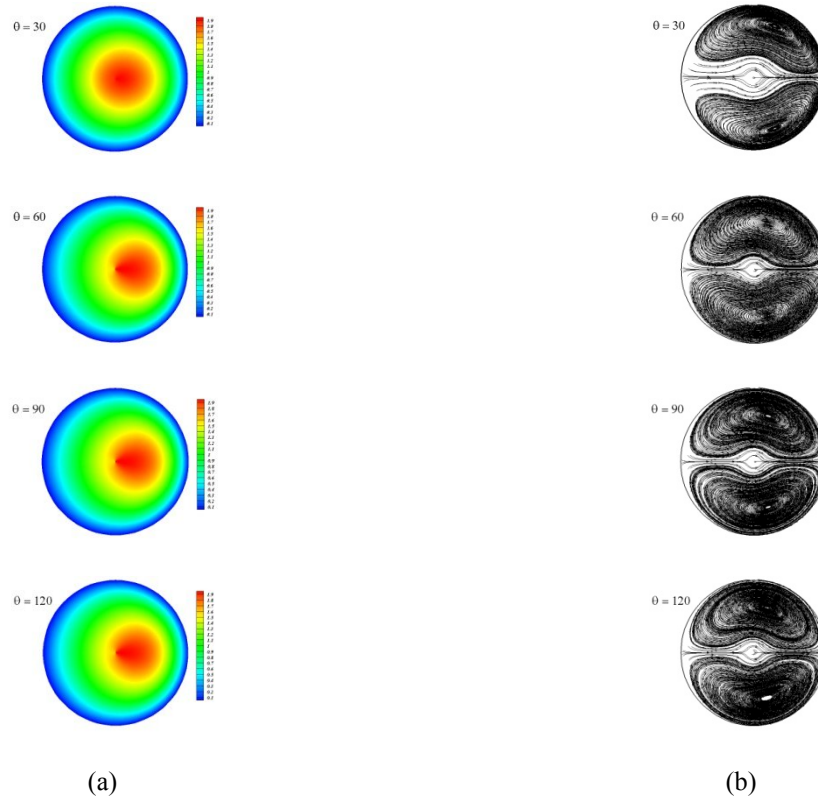(a)   (b)

Fig. 8
(a) Axial velocity contours and (b) secondary streamlines at different sections of the curved vessel, δc=0.1.

In curved paths, centrifugal forces cause the formation of secondary flows and consequently a peripheral boundary layer (similar to the axial boundary layer). Two components of the wall shear stress, one along the vessel axis $\tau r\theta$ and the other in the peripheral direction $\tau r\varphi$, are important. These two components, along with their resultant in the developed region of a curved artery, are shown in Figure 10. As can be seen, the peripheral component of the stress is zero due to the symmetry at angles 0° and 180° and has a maximum value corresponding to the angle corresponding to the center of the Dean vortices. Due to the influx of particles to the outer part of the curvature and the formation of more intense velocity gradients, the value of the wall shear stress is higher in the outer part of the bend ($\varphi = 0°$) and lower in the inner part of the bend ($\varphi = 180°$).

(a)   (b)
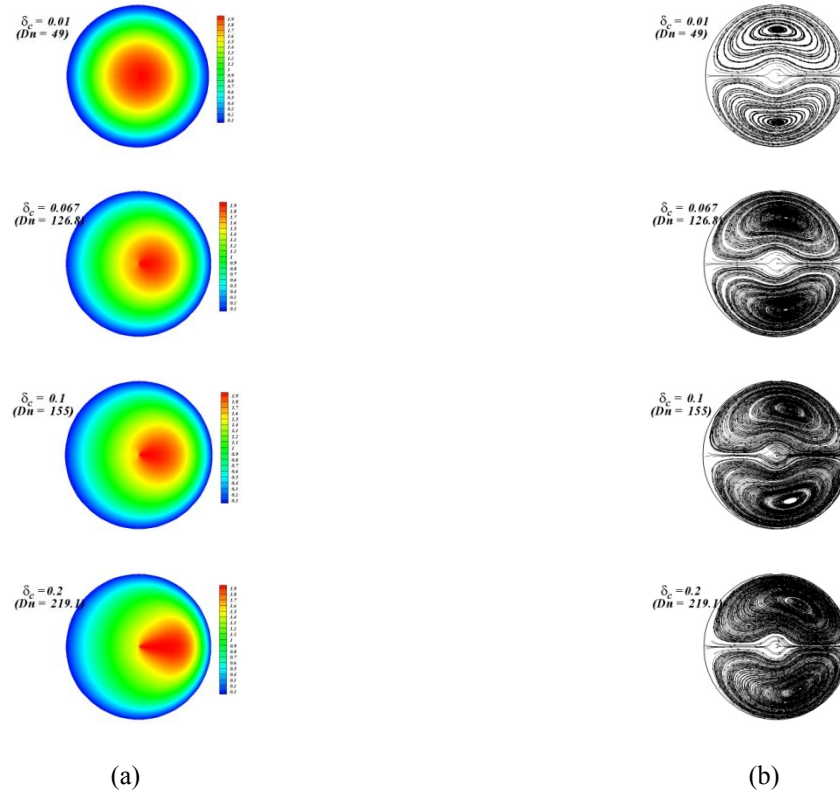
Fig. 9
(a) Axial velocity contours and (b) secondary streamlines in vessels with different curvatures, Re=245.

5.2 LDL Deposition and Diffusion

In this section, the effect of geometric and physiological parameters such as vessel curvature, curvature ratio, and Reynolds number on the distribution of LDL concentration within the blood vessel boundary layer and different layers of the wall, as well as the mass flux rate penetrating into the vessel wall, has been investigated.

Figures 11a and 11b show the changes in the dimensionless surface concentration and dimensionless boundary layer thickness of LDL ($\Delta+=\Delta/R$) in a cross-section for different curvature ratios. According to Figure 11, both parameters decreased in the outer part of the bend and increased in the inner part. As expected, with increasing vessel curvature ratio, these parameters will experience more severe changes in a given cross-section.
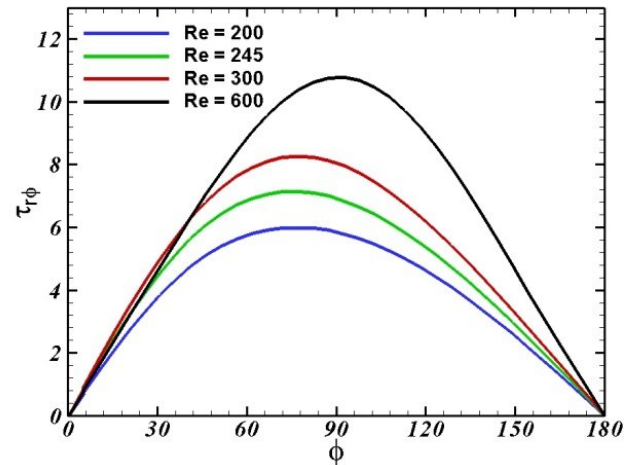
(a)
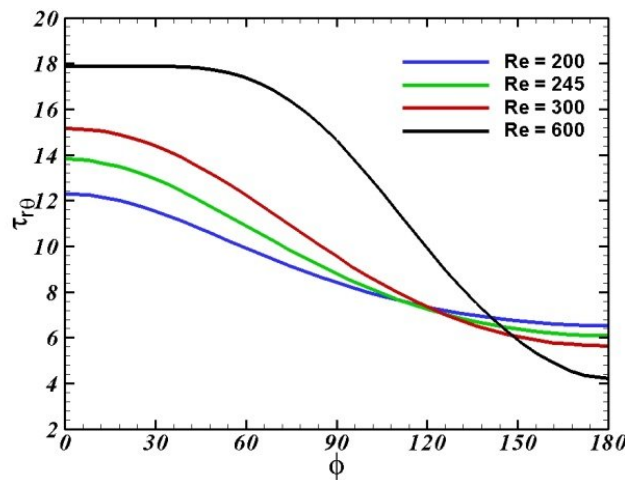
(b)
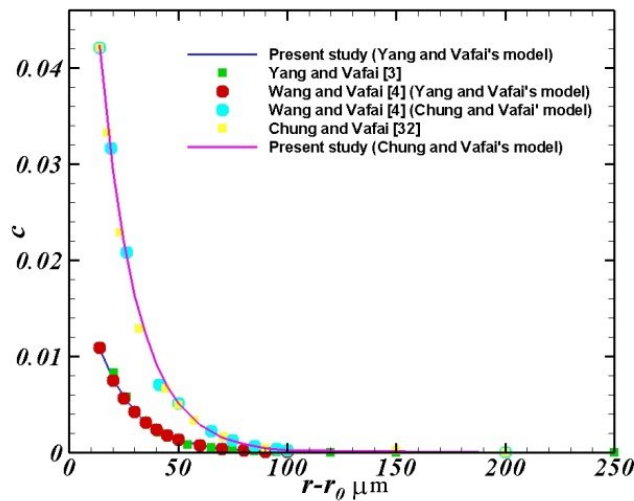
(c)

Fig. 10
(a) Circumferential component, (b) axial component, and (c) resultant wall shear stress in a curved artery, δc=0.1.
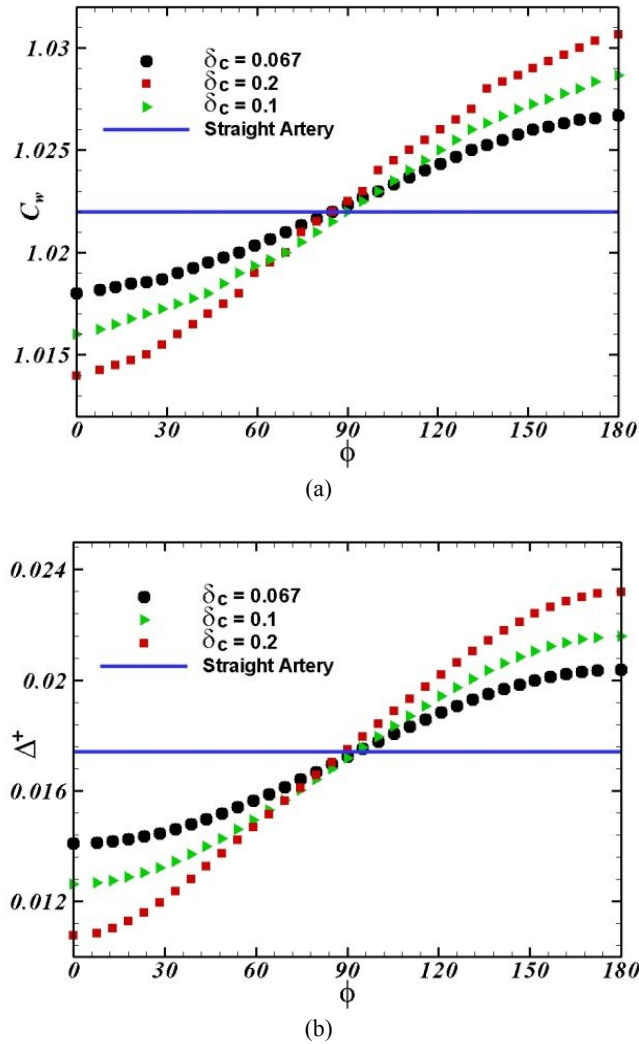
Fig. 11
(a) Surface concentration and (b) boundary layer thickness of LDL concentration in vessels with different curvatures, Re=245.
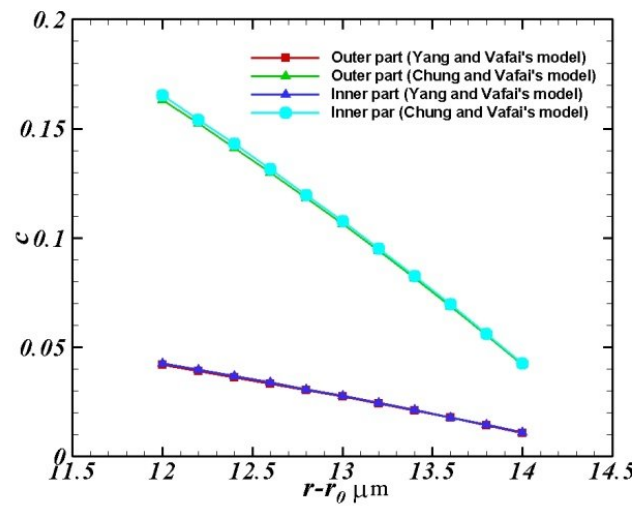
The effect of artery curvature on the concentration distribution of LDL particles in the different layers forming the artery wall is depicted in Figure 12. Due to the higher surface concentration in the inner part of the curvature, the concentration distribution in the endothelium layer in this part increased by about 1.5%, and these changes gradually disappeared in the subsequent layers, so that in the last layer the concentration distribution was almost independent of the vessel curvature. The results confirm the assumption that the wall layers are straight due to their small thickness. It should be noted that, considering the formation of the initial plaque nuclei in the intima layer, a detailed study of the concentration distribution and the effect of various factors on it is very important. As can be seen, the concentration distribution in this layer has a very gentle slope and its input and output fluxes are almost the same under normal conditions.
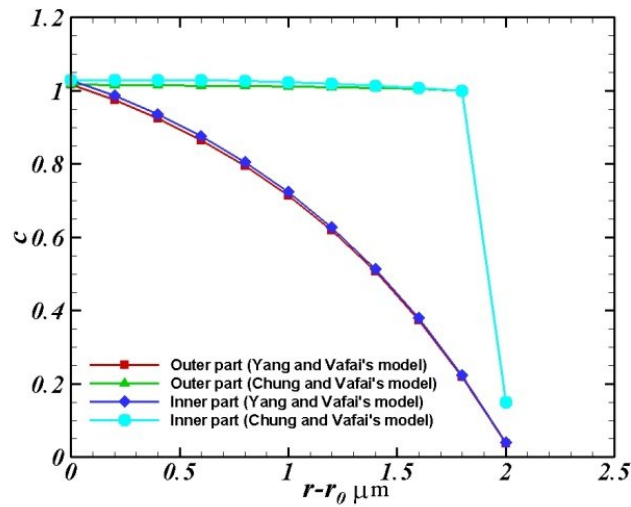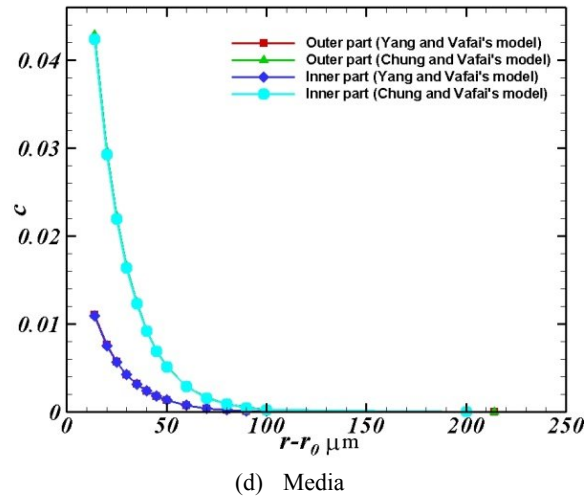
(a) Endothelium

(b) Intima

(c) IEL

(d) Media
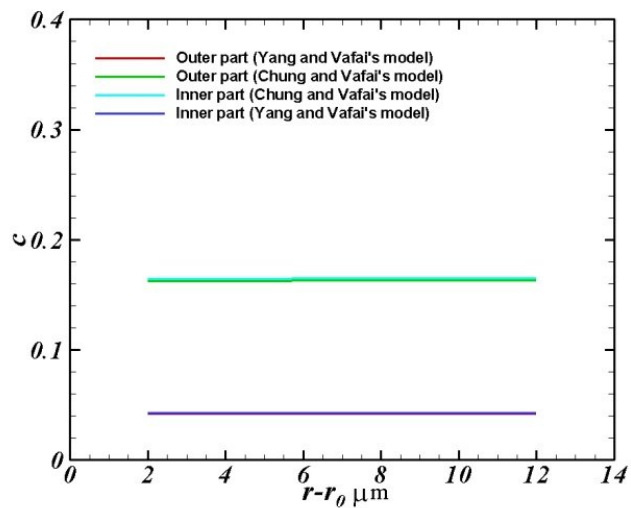
Fig. 12
Effect of arterial curvature on the transverse distribution of LDL concentration in different layers of the curved arterial wall, δc=0.1.

Figure 13 and Figure 14 show the effect of Reynolds number and Schmidt number on the mass flux rate penetrating the wall, respectively. As the Reynolds number increases and inertial forces become dominant, particles have less opportunity to accumulate around the wall and, as a result, they will have less concentration and penetration. A similar trend is observed for the effect of Schmidt number. The growth of Schmidt number can be due to the decrease in LDL diffusion coefficient and the dominance of momentum diffusion in the blood flow. Changes in the particle flux rate penetrating the wall from different points of a certain cross-section in a curved artery are presented in Figure 15. According to the figure, particles will have more penetration possibility near the inner wall of the bend than the outer wall.
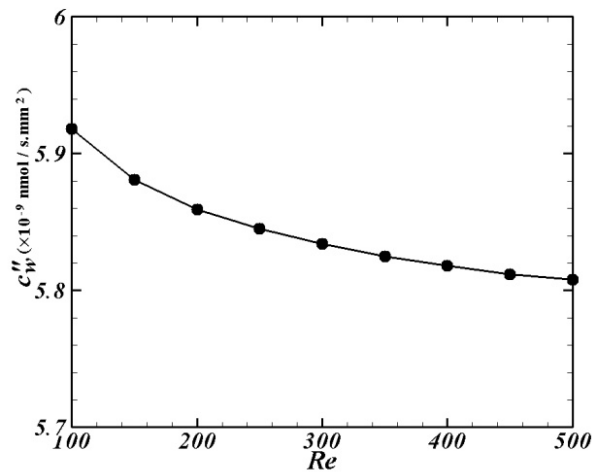

Fig. 13
The effect of Reynolds number on the infiltration flux rate into the curved artery wall, δc=0.1.
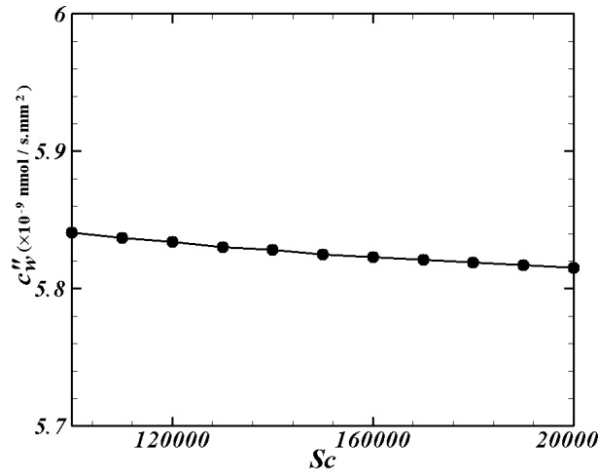
Fig. 14
Effect of Schmidt number on the infiltration flux rate into the wall of a curved artery, δc=0.1.
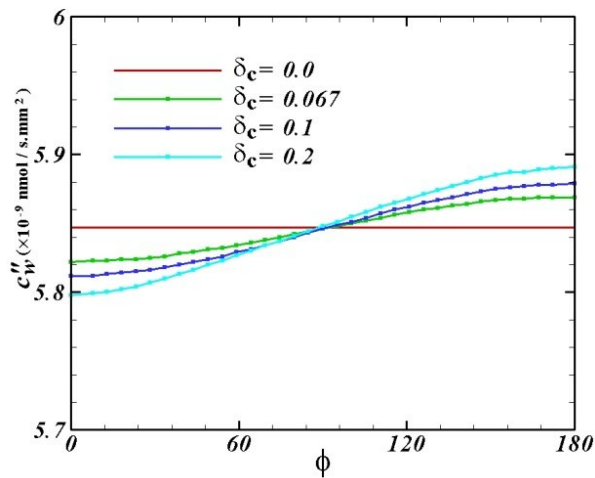

Fig. 15
Effect of arterial curvature on the rate of LDL penetration into the wall, *Re*=245.

The effect of vessel curvature on the distribution of LDL concentration in the boundary layer of a curved coronary artery is shown in Figure 16 and at various points of a given cross-section in Figure 17. In arteries with less curvature, more LDL particles accumulate near the wall, creating a thicker boundary layer. In addition, due to the greater inertia in the outer part of a given curved artery, the boundary layer formed in these areas was much thinner than on the opposite side. In other words, wherever the thickness of the boundary layer is greater, a greater concentration of particles in the wall and a greater rate of their penetration are also observed. In fact, the formation of this very thin layer, which is also called the concentration polarization region, enhances and facilitates the penetration of fat particles into the vessel.
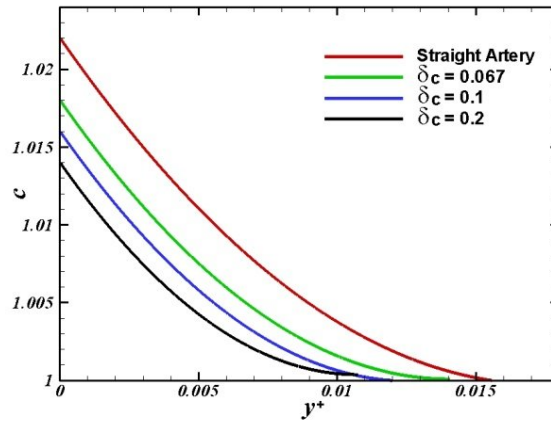
Fig. 16
The effect of arterial curvature on the distribution of LDL concentration in the blood vessel boundary layer, Re=245.
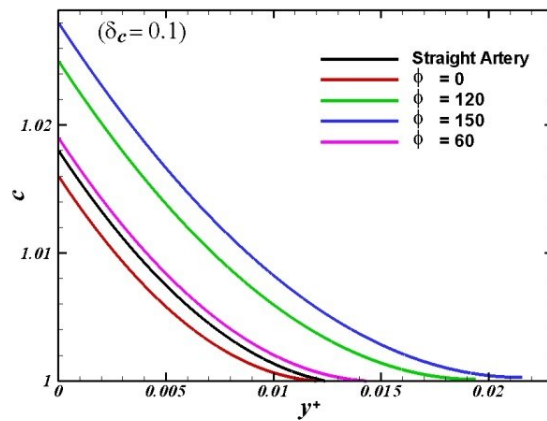

Fig. 17
Distribution of LDL boundary layer concentration at different points of a curved artery cross-section, δc=0.1.
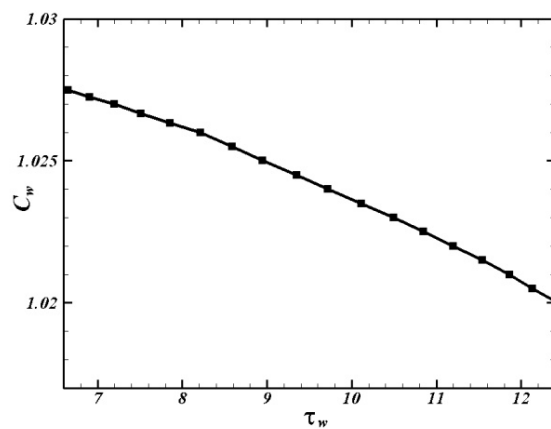
Fig. 18
Changes in LDL surface concentration versus vessel wall shear stress.

Finally, the relationship between LDL surface concentration and wall shear stress is depicted in Figure 18. There is always an inverse relationship between these two parameters. In other words, the points with the lowest wall shear stress in the vicinity of the inner walls of the bends in the blood vessels are the most susceptible areas for the formation and spread of blockages in the vessels.

6   CONCLUSIONS

In this study, LDL mass transport was studied in the lumen and wall of a 120-degree curved coronary artery. This type of vessel is one of the vessels that often become clogged. The main goal of this study was to better understand fluid dynamics, how LDL particles are distributed, their penetration rate, and to discover the points susceptible to complications.

The governing equations, including the continuity equation, momentum conservation, and LDL mass transport, were investigated under the assumption of laminar, incompressible, and Newtonian flow in three dimensions. The effects of physiological parameters such as the vessel curvature ratio, Reynolds number, and Schmidt number on the primary and secondary flow fields, the characteristics of the concentration boundary layer, the mass flux entering the wall, and its distribution in the layers forming the vessel wall were evaluated and measured. In this regard, areas with maximum LDL concentration that are susceptible to the development of atherosclerosis were identified. According to the results, the decrease in the curvature of the vessel and the decrease in the Reynolds number increase the probability of the formation of this disease in the inner wall of the bend. Also, the results showed that the accumulation of LDL particles and their penetration rate into the wall is more intense in the vicinity of the inner part of the curvature than in the outer part. In addition, the effects of the curvature of the vessel on the concentration distribution within the wall layers gradually decay and the direct assumption about them is acceptable with a maximum relative error of 1.5%.

REFERENCES

[1]   Iasiello M, Vafai K, Andreozzi A, Bianco N (2016) Analysis of Non-Newtonian effects on low-density lipoprotein accumulation in an artery. J Biomech 49: 203–209.

[2] Stangeby DK, Ethier CR, (2002) Computational analysis of coupled blood-wall arterial LDL transport. J Biomech Eng 124: 1–8.

[3] Yang N, Vafai K, (2006) Modeling of low-density lipoprotein (LDL) transport in the artery-Effects of hypertension. Int J of Heat and Mass Trans 49: 850–867.

[4] Wang S, Vafai K, (2015) Analysis of low density lipoprotein (LDL) transport within a curved artery. Annal Biomed Eng 43: 1571–1584.

[5] Santra S, Mandal DK, Chakrabarti S, (2018) Effect of pulsatile blood flow on LDL transport in arterial layers. Prog Comput Fluid Dynamics 18: 177–187.

[6] Liu X, Fan Y, Deng X, Zhan F (2011) Effect of non-Newtonian pulsatile blood flow on mass transport in the human aorta. J Biomech 44: 1123–1131.

[7] Wang S, Vafai K (2013) Analysis of the effect of stent emplacement on LDL transport within an artery. Int J of Heat and Mass Trans 64: 1031–1040.

[8] Nematollahi A, Shirani E, Mirzaee I, Sadeghi MR (2012) Numerical simulation of LDL particle mass transport in human carotid artery under steady state condition. Sci Iranica 19: 519–524.

[9] Fazli S, Shirani E, Sadeghi MR (2011) Numerical simulation of LDL mass transfer in a common carotid artery under pulsatile flows. J Biomech 44: 68–76.

[10] Khakpour M, Vafai K (2008) Effects of gender-related geometrical characteristics of aorta-iliac bifurcation on hemodynamics and macromolecule concentration distribution. Int J Heat and Mass Trans 51: 5542–5551.

[11] Prosi M, Zunino P, Perktold K, Quarteroni A (2005) Mathematical and numerical models for transfer of low-density lipoprotein through the arterial walls: a new methodology for the model set up with applications to the study of disturbed luminal flow. J Biomech 38: 903–917.

[12] Fatouraee N, Deng X, De Champlain R, Guidoin R (1998) Concentration polarization of low density lipoprotein (LDL) in the arterial system. Annal New York Academy of Sci 858: 137–146.

[13] Karami F, Hossainpour S, Ghalichi F (2018) Numerical simulation of low-density lipoprotein mass transport in human srterial stenosis-calculation of the filtration velocity. Bio-Med Mat Eng 29: 95–108.

[14] Jesionek K, Kostur M (2015) Effects of shear stress on low-density lipoprotein (LDL) transport in the multi-layered arteries. Int J Heat and Mass Trans 81: 122–129.

[15] Tedqui A, Mallat Z (1999) Atherosclerotic plaque formation. Rev Prat 49: 2081–2086.

[16] Andre P, Baldit SC, Bonneau M, Pigaud G, Hainaud P, Azzam K, Douet L (1996) Which experimental model to choose to study arterial thrombosis and evaluate useful therapeutics?. Haemostasis 26: 55–69.

[17] Xie X, Tan J, Wei D, Lei D, Yin T, Huang J, Qiu J, Tang C, Wang G (2013) In Vitro investigations on the effects of low-density lipoprotein concentration polarization and hemodynamics on atherosclerosis localization in rabbit and zebrafish. J Roy Sci Int DOI: 10.1098/rsif/2012.1053.

[18] Yang N, Vafai K (2008) Low-density lipoprotein (LDL) transport in an artery-A simplified analytical solution. Int J Heat and Mass Trans 51: 497–505.

[19] Nisco GD, Kok AM, Chiastra C, Gallo D, Hoogendoorn A, Migliavacca F, Wentzel JJ, Morbiducci U (2019) The atheroprotective nature of helical flow in coronary arteries. Annal Biomed Eng 47: 519–524.

[20] Roustaei M, Nikmaneshi MR, Firoozabadi B (2018) Simulation of low density lipoprotein (LDL) permeation into multilayer coronary arterial wall: interactive effects of wall shear stress and fluid-structure interaction in hypertension. J Biomech 23: 114–122.

[21] Bukač M, Čanić S, Tambača J, Wang Y (2019) Fluid-structure interaction between pulsatile blood flow and a curved coronary artery on a beating heart: A four stent computational study. Comp Meth Appl Mech Eng 350: 679–700.

[22] Torri R, Oshima M, Kobayashi T, Tagaki K, Tezduyar TE (2009) Fluid-structure interaction modeling of blood flow and cerebral aneurysm: Significance of artery and aneurysm shapes. Comp Meth Appl Mech Eng 198: 3613–3621.

[23] Liu X, Fan Y, Deng X, Zhan F (2011) Effect of non-Newtonian and pulsatile blood flow on mass transport in human aorta. J Biomech 44: 1123–1131.

[24] Deyranlou A, Niazmand H, Sadeghi MR (2015) Low-density lipoprotein accumulation within a carotid artery with multilayer elastic porous wall: Fluid-structure interaction and non-Newtonian considerations. J Biomech 18: 2948–2959.

[25] Iasiello M, Vafai K, Andreozzi A, Bianco N (2017) Analysis of non-Newtonian effects within an aorta-iliac bifurcation region. J Biomech 64: 153–163.

[26] Rabby MG, Razzak A, Molla MM (2013) Pulsatile non-Newtonian blood flow through a model of arterial stenosis. Proc Eng 56: 225–231.

[27] Wada S, Karino T (2002) Theoretical prediction of low-density lipoproteins concentration at the luminal surface of an artery with a multiple bend. Annal Biomed Eng 30: 778–791.

[28] Tamim H, Abbassi A, Fatouraee N (2019) On the effects of straight extremities on low-density lipoprotein transport in the concentration boundary layer of curved arteries. Int J Num Meth Heat Fluid Flow Article in press.

[29] Jesionek K, Kostur M (2015) Effects of shear stress on low-density lipoprotein (LDL) transport in the multi-layered arteries. Int J Heat Mass Trans 81: 122–129.

[30] Nisco GD, Zhang P, Calo K, Liu X, Ponzini R, Bignardi C, Rizzo G, Deng X, Gallo D, Morbiducci U (2018) What is needed to make low-density lipoprotein transport in human aorta computational models suitable to explore links to atherosclerosis? Impact of initial and inflow boundary conditions. J Biomech 8: 33–42.

[31] Akbar NC (2016) Non-Newtonian model study for blood flow through a tapered artery with a stenosis. Alex Eng 55: 321–329.

[32] Chung S, Vafai K (2012) Effect of the fluid-structure interactions on low-density lipoprotein transport within a multi-layered arterial wall. J Biomech 45: 371–381.

[33] Chung S, Vafai K (2014) Mechanobiology of low-density lipoprotein transport within an arterial wall-Impact of hyperthermia and coupling effect. J Biomech 47: 137–147.

[34] Tamim H, Abbassi A, Fatouraee N (2020) Effects of pulsatile flow and straight length on low-density lipoprotein transport in a curved arterial wall. Math Meth Appl Sci Article in press.

[35] Chorin JA (1968) Numerical solution of the Navier-Stokes equations. Math Comp 22: 745–129.